Petroleum Science 22 (2025) 4781–4793

Contents lists available at ScienceDirect

Petroleum Science

journal homepage: www.keaipublishing.com/en/journals/petroleum-science

Original Paper

Coking behavior during the cooling process of cracked hydrocarbon fuels: Characterization of coke and elucidation of condensation coking mechanism

Liu-Ru Liu [a,b], Yu Liu [a,b], Lang Luo [a,b], Xin-Ke Wang [a,b], Wen-Rui Yan [a,b], Bo Wang [a,b,*], Quan Zhu [a,b]

[a] School of Chemical Engineering, Sichuan University, Chengdu, 610065, Sichuan, China
[b] Engineering Research Center of Combustion and Cooling for Aerospace Power, Ministry of Education, Sichuan University, Chengdu, 610065, Sichuan, China

ARTICLE INFO

Article history:
Received 15 December 2024
Received in revised form
23 March 2025
Accepted 11 August 2025
Available online 18 August 2025

Edited by Min Li

Keywords:
Hydrocarbon fuel
Pyrolysis
Condensation
Aggregation
Physical nucleation

ABSTRACT

The active cooling technology of endothermic hydrocarbon fuels is a key way to solve the thermal protection of high-speed aircraft engines, but the condensation coking problem during engine shutdown is a bottleneck that affects the reusability of aircraft. In this study, a self-designed apparatus was used to separately analyze the condensation coking during the fuel cooling process, and the coking characteristics under different temperature conditions were obtained. The condensation coking mechanism of fuel during cooling process was proposed based on the changes in physical properties of coking precursors obtained by the group contribution method. When the temperature drops to 300 °C, not only the gas yield and conversion increase to 71.42% and 89.75% respectively, but the coke mass on the inner surface of the tube also significantly increases from 0.39 to 1.92 mg. Meanwhile, as the temperature further decreases, the morphology of coke gradually transforms into amorphous carbon with a higher degree of graphitization. During the cooling process, due to the liquefaction of coking precursors, their physical properties such as viscosity, density, and saturated vapor pressure undergo sudden changes at 300 °C, leading to enhanced intermolecular physical interactions and promoting the physical aggregation of coking precursor molecules, which are deposited on the inner wall of the tube. This work provides a theoretical basis for the subsequent study of condensation coking mechanisms and inhibition methods.

1. Introduction

In recent years, with the rapid development of aviation and aerospace, industries reusable aircraft has become a major research focus (Kim et al., 2022; Luo et al., 2021; Van et al., 2013; Yan et al., 2024). This technology aims to enable multiple start-stop cycles in engines, requiring high reliability and durability (Ning et al., 2013). However, the issue of carbon deposition during engine shutdown is a significant bottleneck affecting reusability (Gong et al., 2023; Zhang et al., 2024). Accumulated coke during fuel cooling process not only increases the frequency of maintenance and cleaning but also reduce heat transfer efficiency and lead to instability thrust, influencing the multiple cycle use of the engine (Feng et al., 2019; Xiong et al., 2019). Therefore, addressing the carbon deposition issue during the cooling process is critical to achieving reliable engine reusability.

In terms of experimental research, it has been shown that the coking mechanism of hydrocarbon fuels differs significantly at different experimental conditions (Guisnet and Magnoux, 2001; Liu et al., 2021; Zhu et al., 2018). The coking mechanism is primarily categorized into three types: thermal cracking coking, oxidation coking, and catalytic coking (Konda et al., 2022; Shukla and Koshi, 2012; Vuchuru et al., 2023). Thermal cracking coking is the process in which free radicals generated from the pyrolysis continuously dehydrogenate and polymerize to form coke

* Corresponding author.
E-mail address: bo.wang@scu.edu.cn (B. Wang).
Peer review under the responsibility of China University of Petroleum (Beijing).

https://doi.org/10.1016/j.petsci.2025.08.019

Nomenclature

v	coking rate, mg·m^2·s^{-1}
A	cross-sectional area, m^2
T	unit time, s
y	gas yield, %
m_l	total mass of liquid products, g
m	total mass of reactant, g
$m_{reacted}$	total consumption mass of reactant, g
X	conversion rate, %
p	pressure, MPa
p_c	critical pressure, MPa
V	molar volume, m^3/mol
V_c	critical molar volume, m^3/mol
T	temperature, K
T_b	boiling temperature, K
T_c	critical temperature, K
T_{br}	T_b/T_c
T_r	reduced temperature
p_{vpr}	reduced vapor pressure
N_k	total number of kth groups
tck	contribution to critical temperature
pck	contribution to critical pressure
tbk	contribution to critical boiling temperature
vck	contribution to critical molar volume
N_{atoms}	total number of atoms
a, b	parameters in PR EoS
$\overline{M}$	molecular weight, g/mol
R	universal gas constant, J/(mol·K)
$f^{(0)}$,$f^{(1)}$,$f^{(2)}$	parameters in Ambrose-Walton equation
N	molecular number per unit volume, mol/m^3
$\bar{v}$	average velocity of molecules, m/s
D	effective diameter of molecules, m
Z	average collision frequency, s^{-1}

Greek symbols

P	density of fluid, g·cm^{-3}
M	viscosity of fluid, mPa·s
η^*	viscosity correction factor
ω	acentric factor

Subscripts

c	critical
l	liquid products
k	groups type

deposits. Oxidation coking is mainly caused by the self-oxidation reaction of dissolved oxygen in the fuel to form coke. Catalytic coking is mainly the process that coking precursors continuously grow into coke under the catalysis of metals (Chen et al., 2024; Richter and Howard, 2000; Wang et al., 2025).

In order to further explore the coking mechanism, numerous scholars have conducted detailed simulation studies of these processes, founding that the nucleation and aggregation of small molecules are identified as critical steps in coke formation (Gleason et al., 2021; Morán et al., 2021; Song et al., 2009; Wang et al., 2023; Yin et al., 2023; Yuan et al., 2019; Zhang et al., 2023; Zhao et al., 2021). Based on the different aggregation principles of coking precursor molecules (DeWitt et al., 2011, Wang et al., 2021a), three nucleation modes have been identified: physical nucleation, non-nucleation, and chemical nucleation (Chung and Violi, 2011; Mao et al., 2017). At present, due to limitations of experimental equipment, it is difficult to obtain coking pathways through experiments (Liu et al., 2015; Sharma et al., 2021; Sun et al., 2017), which has led many scholars to obtain coking characteristics through thermodynamic and kinetic. During pyrolysis and coking processes, the different structural characteristics of coke, such as pore structure and microscopic anisotropy, can lead to changes in adsorption thermodynamic parameters (Efimov et al., 2024; Litvinova et al., 2024). In addition, the pyrolysis kinetics model is directly related to the rate and mechanism of coking process (Sharikov et al., 2023).

Although the studies mentioned above have illuminated the mechanisms of fuel coking at various temperatures during heating, there are still some differences in the coking behavior between the high-temperature process and the cooling process of fuel. Currently, research on this cooling-process coking behavior is relatively limited. Studies have shown that the coking behavior of asphaltene molecules during cooling is different from that during pyrolysis. Asphalt molecules undergo different aggregation patterns with different cooling rates (Khalaf and Mansoori, 2018; Yu et al., 2023). Meanwhile, the coking behavior of fuel during the cooling process is closely related to the products during the fuel pyrolysis and the material of tube. The content of cracking products (methane and ethane) can affect the molecular aggregation rate, and the different wall energies of the tube can affect the rate at which molecules aggregate and deposit on the tube wall (Liu et al., 2023; Wang et al., 2024). The coking behavior of fuel during the cooling process has been demonstrated, however, the coking mechanism of the cooling process of high temperature fuels still needs to be further investigated.

A large number of high-temperature coking experiments have shown that unstable system pressure during the cooling process can lead to tube blockage, affecting the system to undergo multiple cycles, as shown in Fig. S1. Therefore, there is an urgent need for a new experimental method to study the fuel coking process during cooling and elucidate potential coking mechanisms.

This article uses a self-designed device to separate the high-temperature cracking and cooling processes, in order to obtain the coke produced during the cooling process, and measure its quality, morphology, and elemental distribution. By using the group contribution method and Fortran physical property calculation method to track the changes in the physical properties of coking precursors, the potential coking mechanism of fuels during the cooling process is further revealed. This study provides a new perspective for solving the coking problem during the fuel cooling stage and lays the foundation for improving the long-term reusability of engines.

2. Experimental and calculation methods

2.1. Experimental materials and apparatus

Chinese No. 3 jet fuel (RP-3) is a typical aviation fuel, and n-decane is one of the main components of RP-3 (Abdalla et al., 2020; Huang et al., 2023; Mao et al., 2019). Therefore, n-decane (mass fraction >99%) was used as a substitute for aviation kerosene in this study. The thermal cracking section tube (inner diameter 2 mm, length 800 mm) and the condensation section tube (inner diameter 4 mm, length 420 mm) used in the experiment are both made of SS304 stainless steel material. The

experimental system is shown in Fig. 1, and the experimental conditions are displayed in Table 1.

This experimental device is used to study the characteristics of coke formation during fuel cooling process, which is divided into high temperature section and cooling section. An electric heating system in the high-temperature section is used to simulate the thermal cracking process of fuel. A self-made condenser is used to simulate the formation of coke during the cooling process. Throughout the entire experiment, the condensing medium is continuously introduced into the device at a constant flow rate through a high-pressure constant flow pump to ensure the cooling rate of the fluid. There are two buckles designed at both ends of the condenser tube. After the experiment is completed, the reaction tube can be disassembled for subsequent characterization of the coke, as shown in Fig. S2.

2.2. Analysis of cracking products

2.2.1. Thermal cracking of n-decane

Gas chromatography was used to determine the pyrolysis products of *n*-decane at different outlet temperatures. The gas yield (y) refers to the ratio of the gas mass to the total mass of the gas-liquid phase products per unit time. It is a key indicator for evaluating the degree of fuel cracking during the pyrolysis process and is defined as follows:

$$y = 1 - m_l/m \tag{1}$$

The conversion rate (x) is defined as the ratio of the mass of reactant reacted to the total mass of reactant in the cracking reaction, as shown in Eq. (2):

$$x = m_{\text{reacted}}/m \tag{2}$$

2.2.2. Coke characterization

In this experiment, the coke mass along on the inner wall of the tube was measured using the oxidation method. As shown in Fig. 2, the coke of the reaction tube reacts with oxygen to be oxidized into carbon dioxide. By employing the Lambert-Beer absorption law, the concentration of carbon dioxide is ultimately calculated, determining the mass of coke.

The coking rate (v) is defined as the mass of coke formed per unit area per unit time and is calculated using the following formula:

$$v = m_C/At \tag{3}$$

To further observe the differences of coking under various conditions, Scanning Electron Microscope (SEM), Energy Dispersive Spectroscopy (EDS), and Raman spectra were employed to characterize the morphology, elemental composition, and graphitization degree of the coke.

2.3. Calculations of key properties

2.3.1. Critical parameters

The critical parameters of a substance are prerequisites for the forming of the coefficients a and b in the PR EoS, and are also key parameters for calculating the physical properties of substances (viscosity, density, and saturated vapor pressure). For stable or metastable species, these parameters can easily be obtained through experimental measurement or from published literature and data. However, for most coking precursors, experimental measurement is challenging and estimates are required. Given knowledge of the chemical structure of a species, group contribution methods are widely regarded as the most reliable estimation methods, such as those suggested by Constantinou (Constantinou and Gani, 1994), Fedors (1982), and Joback (Joback and Reid, 1987), as illustrated in Fig. 3.

This research utilizes the Joback method for estimating critical temperature, critical pressure, and critical volume, providing critical parameters for subsequent physical property calculation. The formulas are as follows:

$$T_c = T_b\left[0.584 + 0.965\left\{\sum_k N_k(tck)\right\} - \left\{\sum_k N_k(tck)\right\}^2\right]^{-1} \tag{4}$$

$$p_c = \left[0.113 + 0.0032N_{\text{atoms}} - \left\{\sum_k N_k(pck)\right\}\right]^{-2} \tag{5}$$

$$V_c = 17.5 + \sum_k N_k(vck) \tag{6}$$

It is worth noting that the calculate of T_c requires the standard boiling point T_b of the substance, which can be estimated using the Joback method.

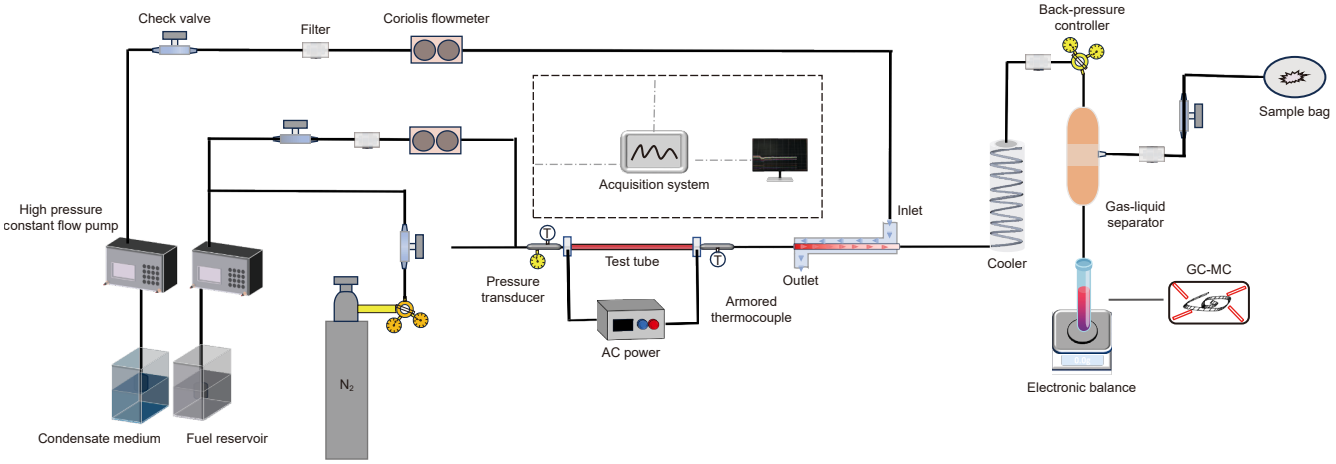

Fig. 1. Apparatus of supercritical hydrocarbon fuel pyrolysis and coking experiment.

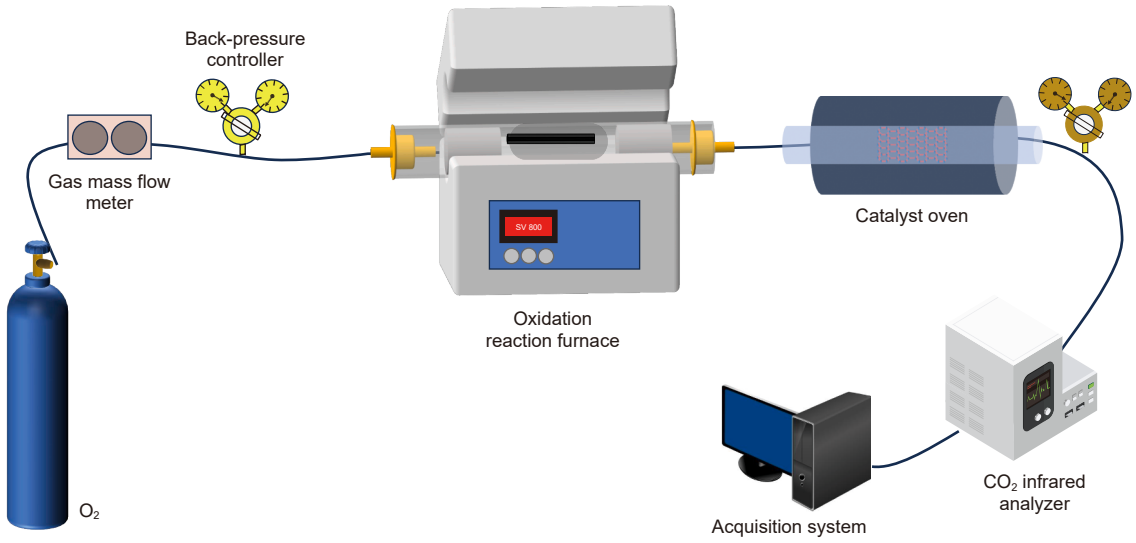

Fig. 2. Experimental facility for coke mass analysis.

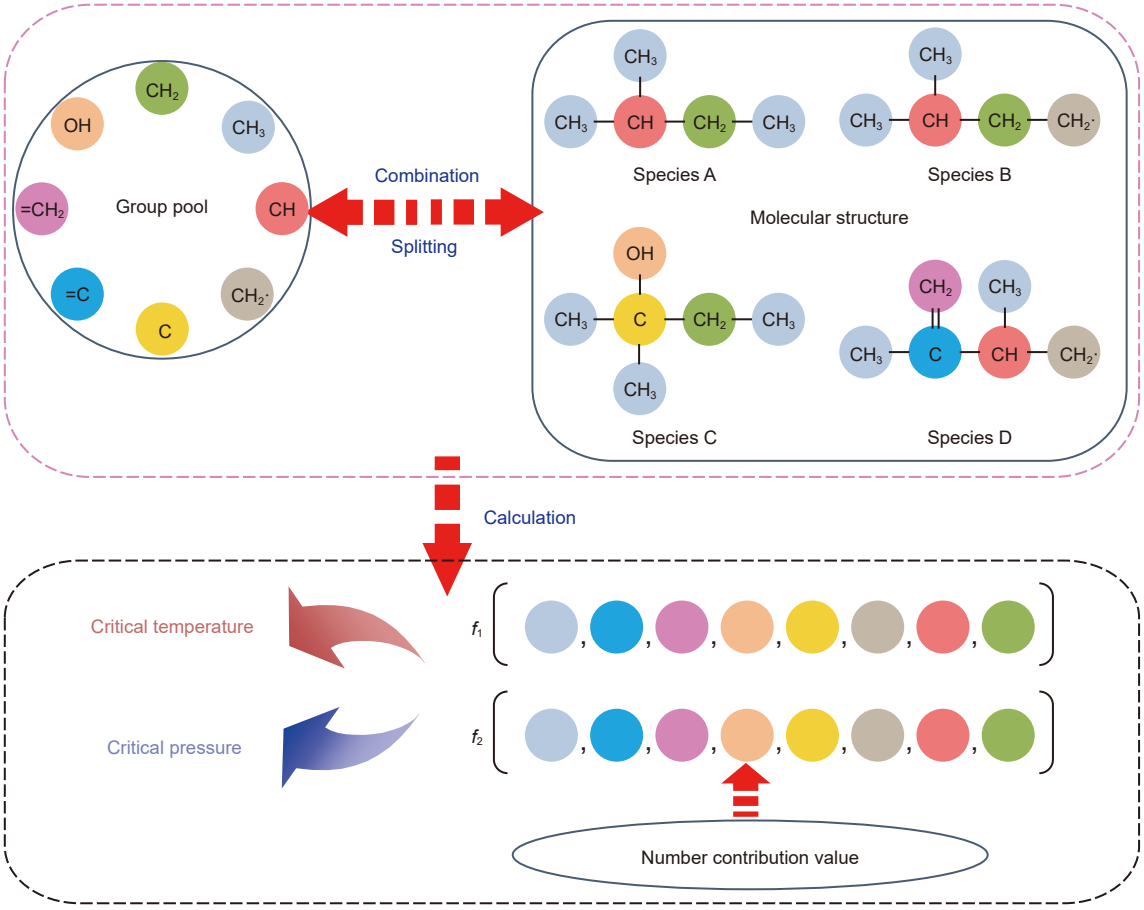

Fig. 3. Schematic diagram of group contribution method.

$$T_b = 198 + \sum_k N_k(tbk) \quad (7)$$

2.3.2. Viscosity and density

For high-pressure processes, the ideal gas equation of state is no longer suitable for measuring the density of substances. Cubic

equations of state (EoS) are often used to describe the pressure-volume-temperature (P-V-T) relationships of high-pressure fluids, due to the simple form and good predictive ability for large-scale fluid properties. Consequently, for this study, we chose to use the Peng-Robinson (P-R) equation of state to measure the density of substances (Peng and Robinson, 1976).

$$p = \frac{RT}{(\overline{M}/\rho - b)} - \frac{a}{(\overline{M}/\rho)^2 + 2b(\overline{M}/\rho) - b^2} \tag{8}$$

$$a = \frac{0.457247R^2T_c^2}{p_c}\left[1 + j\left(1 - \sqrt{\frac{T}{T_c}}\right)\right]^2 \tag{9}$$

$$b = \frac{0.0778RT_c}{p_c} \tag{10}$$

$$j = 0.37464 + 1.5422\omega - 0.26992\omega^2 \tag{11}$$

Viscosity is a direct result of molecular collisions, and accurate calculation of material viscosity is crucial in the phase transition process. The viscosity of fluids under supercritical conditions is calculated using the method proposed by Chung et al. (1984), which employs empirical correction factors to account for the impact of high fluid density on viscosity. The primary equation for calculating viscosity in this method is:

$$\mu = \eta^* \frac{36.344(MT_c)^{1/2}}{V_c^{2/3}} \tag{12}$$

η^* is a parameter related to the fluid density and specific volume. The methods for calculating the parameter can be found in Tables S1 to S3.

2.3.3. Saturated vapor pressure

Three-parameter corresponding states method proposed by Ambrose and Walton is used to calculate saturated vapor pressure (Ambrose and Walton, 1989), which offers high accuracy for hydrocarbons. The saturated vapor pressure based on critical temperature (T_c), critical pressure (p_c), and acentric factor (ω) is calculated as follows:

$$\ln p_{vpr} = f^{(0)} + \omega f^{(1)} + \omega^2 f^{(2)} \tag{13}$$

$$\omega = \frac{-\ln(p_c/1.01325) + f^{(0)}(T_{br})}{f^{(1)}(T_{br})} \tag{14}$$

$$f^{(0)} = \frac{-5.97616\tau + 1.29874\tau^{1.5} - 0.60394\tau^{2.5} - 1.06841\tau^5}{T_r} \tag{15}$$

$$f^{(1)} = \frac{-5.03365\tau + 1.11505\tau^{1.5} - 5.41217\tau^{2.5} - 7.46628\tau^5}{T_r} \tag{16}$$

$$f^{(2)} = \frac{-0.64771\tau + 2.41539\tau^{1.5} - 4.26979\tau^{2.5} + 3.25259\tau^5}{T_r} \tag{17}$$

$$\tau = 1 - T_r \tag{18}$$

3. Results and discussion

3.1. Cracking characteristics

The cracking characteristics were analyzed to explore the impact of cooling process on fuel cracking, as displayed in Fig. 4. Gas yield and conversion of fuel are indirect indicators reflecting the depth of fuel pyrolysis. As shown in Fig. 4(b), when the condensation temperature is 600 °C, the gas yield and conversion are 65.46% and 86.36%, respectively. As the temperature drops to 300 °C, these two indicators are 71.42% and 89.75%, respectively. The system pressure remains constant, and the gas yield and conversion slightly increase with the decrease of temperature. Under these conditions, the density and viscosity of the pyrolysis products will also increase. This will result in a decrease in flow rate and an increase in residence time, and ultimately promote fuel cracking.

Fig. 4(c) shows the mole fraction changes of gas products at different outlet condensation temperatures. Among them, the content of methane and propylene shows the most significant change. As the temperature decreases, the methane content first decreases from 29.48% to 21.21% and then increases to 26.06%, while the trend of propylene is completely opposite, increasing from 11.24% to 16.48% and then decreasing to 13.05%.

The highly active small molecules produced by cracking are easily combined to form methane. However, propylene, as an intermediate in the reaction, is easy to undergo secondary reactions and further converted into other substances during the cooling process. Under high temperature conditions, fuel undergoes cracking to produce a large amount of small molecule substances. As the cracking reaction continues to deepen, secondary reactions will occur, and some products will further crack to other substances (Vandewiele et al., 2014, Wang et al., 2021b). Propylene, as an unsaturated hydrocarbon in cracking reactions, has high reactivity due to its unsaturated structure. Double bonds are easily broken again or react with other molecules to form smaller and more stable molecules (such as ethylene and methane). Methane increases relatively at lower temperatures due to its simple and stable properties.

In this study, only the key liquid phase that affect the coking process are discussed. Fig. 4(c) shows the mass fraction changes of main liquid-phase products at different outlet condensation temperatures, which are also the primary coking precursors. As the temperature decreases, the mass fraction of benzene first decreases from 60.06% to 50.97%, and then increases to 57.55%. In addition, although the mass fractions of 1,4-cyclohexene and cyclohexene are small, the trend of content change is the same as that of benzene.

These changes indicate that condensation has a significant impact on the cracking products and their conversion processes. In order to further study the effect of condensation on coking, this article analyzes the coking products produced at different condensation temperatures through coking experiments and explores their influence on coking formation. In future research, molecular dynamics simulations will be combined to conduct the analysis of the thermodynamics and kinetics of condensation coking in depth (Jia et al., 2014).

3.2. Coking characteristics

Coking experiments with different outlet condensation temperatures were conducted under conditions of the flow rate of 1 g/

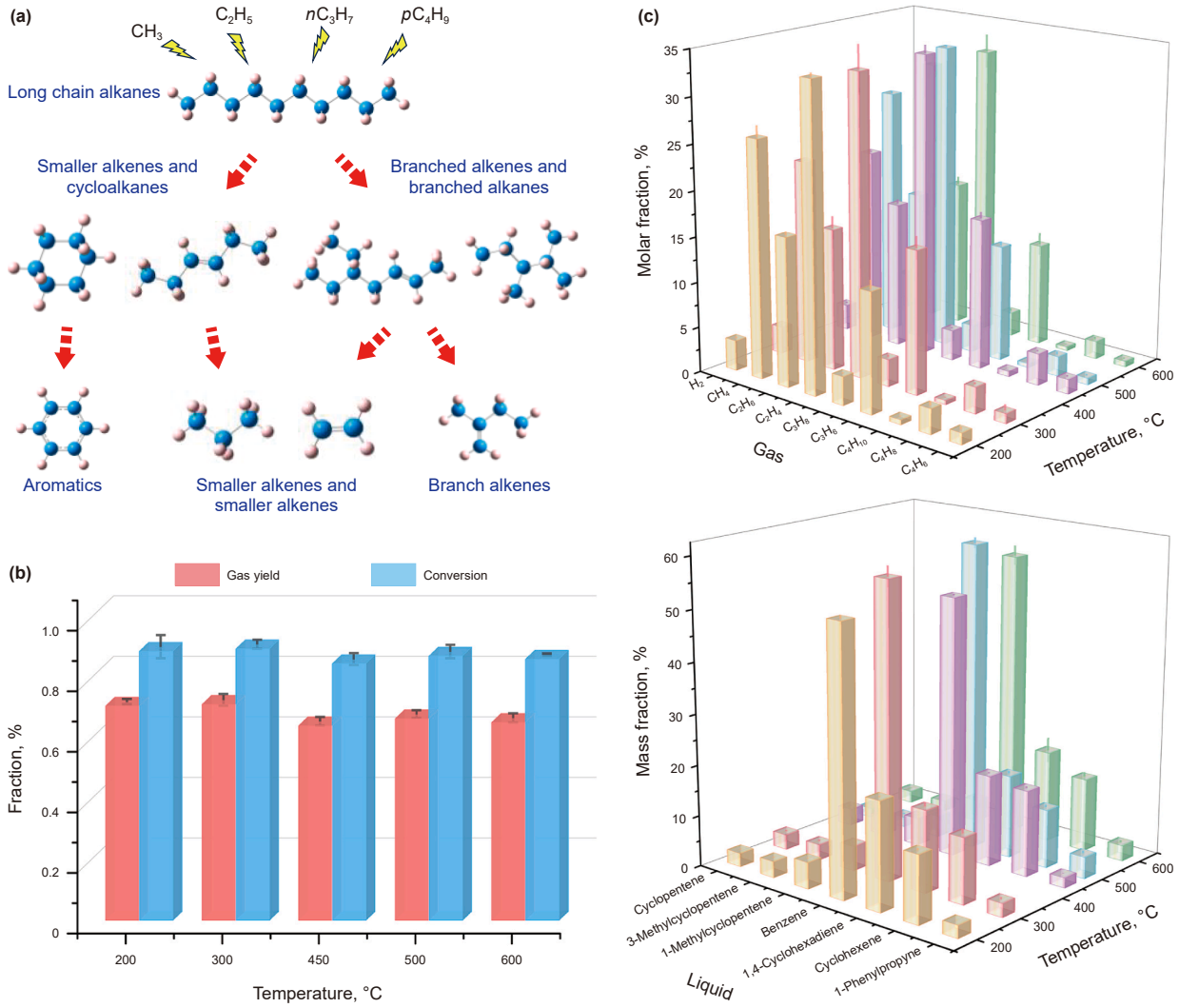

Fig. 4. (**a**) Schematic diagram of *n*-decane fuel cracking; (**b**) gas yield and conversion; (**c**) the mass of gas-phase products and the mole fraction of liquid-phase products (coking precursor) under different condensation conditions.

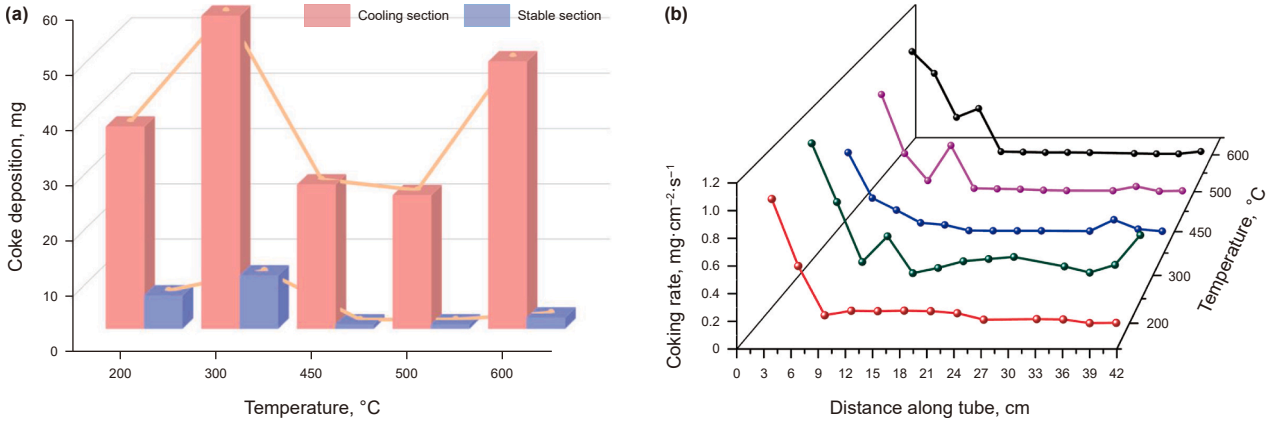

Fig. 5. The distribution of coke at different outlet condensation temperatures: (**a**) coking mass; (**b**) coking rate along the tube.

s and the coking duration of 10 min. As shown in Fig. 5, the mass of coke deposits is significantly affected by the changes in port flow rate, and the data fluctuates greatly and remains unstable. Therefore, the middle section of 12–33 cm is more suitable for exploring the coking in the cooling process.

During the cooling process, the total mass of coke exhibits a trend of first decreasing, then increasing and finally slow decreasing as outlet condensation temperature decreases. Specifically, as the condensation temperature decreases from 600 to 450 °C, the coke mass along the tube decreases from 0.39 to

0.15 mg, and the coking rate decreases from 0.021 to 0.008 $mg \cdot cm^{-2} \cdot s^{-1}$. However, as the temperature further decreases to 300 and 200 °C, the coke mass and coking rate increase sharply, reaching 1.92 and 1.20 mg, 0.102 and 0.064 $mg \cdot cm^{-2} \cdot s^{-1}$, respectively.

It should be pointed out that the coke mass and coking rate of coke produced at 200 °C are lower than those at 300 °C, which may be attributed to differences in cooling rates. When the tube length and cooling inlet temperature are the same, the lower fuel temperature indicates the faster cooling rate. When the cooling rate is fast, the fuel stays in the high-temperature region for a shorter period of time, producing fewer coking precursors. Similarly, when hydrocarbon fuel enters the condenser tube, the fuel temperature changes rapidly in a short period of time, resulting in unstable fuel flow inside the tube. Therefore, there is a peak in coking mass.

The mass of coke increases as the condensation temperature decreases, probably due to physical aggregation of coking precursors. Coking precursors refer to substances that can occur chemical reactions to form coke. To further understand the aggregation of precursors during the cooling process, the critical temperature parameters of the main coking precursors were obtained using Fortran programming based on the physical property calculations and critical property estimation methods described in section 2.3, as shown in Table 2.

Table 2 lists the critical temperature of several common coking precursors at the pressure of 3.5 MPa, which is also the maximum temperature allowed for gas liquefaction. Under this pressure condition, the critical temperature of most coking precursors is within the range of 200–300 °C. But below this temperature, a phase change occurs, altering physical properties (including viscosity, density, etc.), thereby affecting the fuel pyrolysis and coking process of the fuel. This also tentatively explains the phenomenon of high coke mass at the range of 200–300 °C in Fig. 5.

To further investigate the impact of condensation on the coking process, techniques such as SEM and EDS were used to explore the micro-morphology and elemental composition of coke deposits on the inner walls of microchannels, and the coke characteristics were further analyzed. This analysis aims to reveal the differences between condensation coking and cracking coking, providing a basis for constructing a coking mechanism of fuel during the cooling process.

Fig. 6(a) shows the morphology of coke deposits during two different stages of high-temperature cracking and cooling. Under the fuel cracking at high temperature of 750 °C, coke is basically spherical carbon. At medium temperatures of 450 and 500 °C, the coke morphology is primarily filamentous carbon. As the temperature is further reduced to 200 and 300 °C, the coke mainly exhibits the amorphous structure.

The results indicate that there are significant differences in the morphology of coke produced at different temperatures. During the cracking process, the coking is mainly in the form of bulk phase coking. The free radicals generated after fuel cracking undergo addition reactions to form PAHs, which further grow into particles or spherical coke through dehydrogenation reactions. As the condensation temperature decreases, the coking is mainly metal catalytic coking. Under the catalytic action of active metals such as iron (Fe) and nickel (Ni), a large number of filamentous carbons are formed on the surface of the substrate, until the active sites are covered and deactivated. As the temperature further decreases, the coking precursor undergoes liquefaction and its physical properties change. The molecules interaction leads to the random aggregation of molecules. With the continuous aggregation and accumulation of molecules, large molecular clusters are eventually formed and deposited on the tube wall, resulting into the formation of amorphous coke.

Table 1
Experimental parameters of the cooling process.

Conditions	Value
Mass flow, g/s	1.0
Inlet fuel temperature, °C	750
Outlet fuel temperature, °C	200, 300, 450, 500, 600
System pressure, MPa	3.5
Cooling section length, mm	420

Table 2
The critical temperature parameters of the main coking precursors.

Substance	T_c, °C
Cyclopentene	233.0
3-Methylcyclopentene	235.9
1-Methylcyclopentene	235.0
Benzene	289.5
1,4-Cyclohexadiene	264.8
Cyclohexene	287.4
1-Phenylpropyne	405.9

EDS was used to acquire the elemental analysis of the coke, as shown in Fig. 6(b). Elemental analysis of the coke produced by the fuel cracking reveals that the content of carbon element accounts for about 97.51%. Meanwhile, almost no signals of metal elements are detected, indicating that a certain thickness of coke layer is formed. However, from the observations of the production of coke during the cooling process, the iron content in the coke layers reaches about 50%, even exceeding 55% at the condensation temperature of 200–300 °C, suggesting that the coke layers formed under these conditions are relatively thin.

Comparing the distribution of coke mass during the cooling process shown in Fig. 5, the coke mass is significantly higher at 200–300 °C than that of other condensation temperatures. In order to further verify the elemental distribution of coke, EDS point measurements were performed on these two temperatures. It is found that the carbon element content at 200 and 300 °C is about 82.3% and 84.8%, which are 9.4 times and 8.0 times higher than that of surface scanning, respectively.

This finding reveals the coke formed during the cooling process is not as uniform as the coke produced during the thermal cracking. The coke formed during the cooling process is more concentrated at a certain position on the pipe wall, while the coke produced during the thermal cracking process uniformly adheres to various positions on the pipe wall. The inhomogeneity of coke produced by cooling may mainly be caused by the physical aggregation of coking precursors.

Raman spectroscopy is a highly effective tool for detecting the degree of graphitization of coke, with the D and G peaks being the most important characteristic peaks. The peak area ratio (I_D/I_G) of the D and G peaks can be obtained by peak fitting. In carbon materials, graphitization degree refers to the degree of ordered arrangement of carbon atoms in coke. The I_D/I_G value can be used as a quantitative indicator of the degree of graphitization. A lower I_D/I_G value indicates a stronger G peak, and the graphite structure in the coke is more ordered with a higher degree of graphitization.

Fig. 6(c) shows the changes in the graphitization degree of coke under different conditions. The I_D/I_G values of coke produced by the fuel cracking reaches above 2.8, indicating that the coke have low graphitization degree. As the condensation temperature gradually decreases, the graphitization degree of coke produced by the cooling process increases. When the condensation temperature of 200–300 °C, the I_D/I_G values of coke are around 2.0.

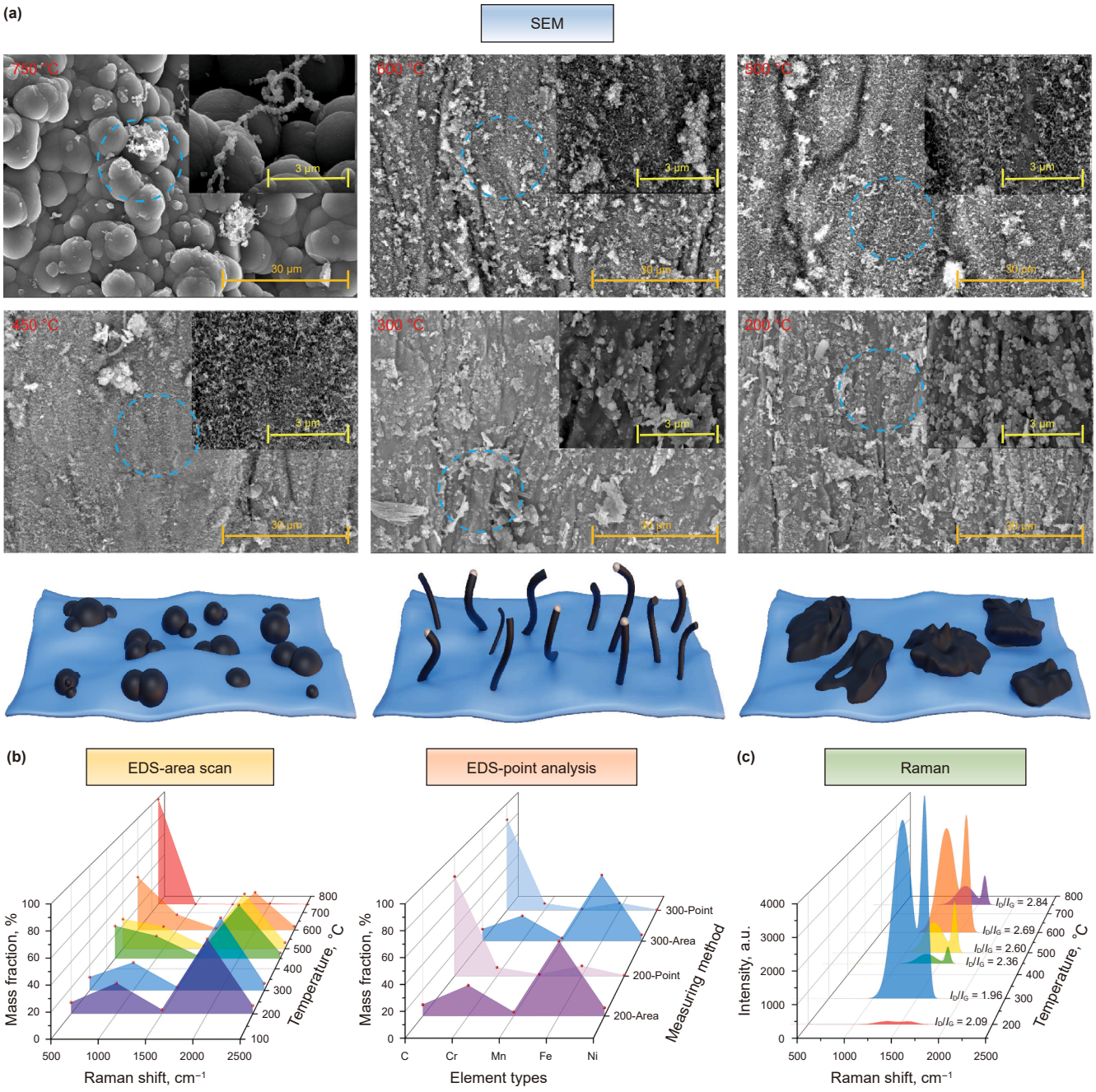

Fig. 6. Characterization of coke obtained at the cracking temperature of 750 °C and different condensation temperatures of 600, 500, 450, 300 and 200 °C, respectively. **(a)** SEM image; **(b)** EDS scan; **(c)** Raman spectral.

During the thermal cracking process, the coking precursor is in a gaseous state, resulting in violent molecular motion and disordered arrangement of carbon atoms (Miroshnichenko et al., 2023). The structure of coke contains more defects and irregularities, resulting in poor hardness, strength, and wear resistance, as well as lower electrical and thermal conductivity. Therefore, the graphitization degree of coke is low. On the contrary, during the cooling process, due to the liquefaction of the coking precursor, the molecular interactions increase, and the carbon atoms are arranged in an orderly manner (Heintz, 1985). It exhibits better hardness, strength, wear resistance, as well as higher electrical and thermal conductivity, resulting in a higher graphitization degree of the coke.

The properties of coke are closely related to the degree of graphitization. As the temperature gradually decreases, it transforms into a liquid state and the molecular interactions increase. Carbon atoms gradually arrange in an orderly manner, forming stable and strong covalent bonds. Therefore, the hardness and strength of coke is enhanced, which is difficult to deform when subjected to external forces. In the graphite structure, carbon atoms form a stable hexagonal network, in which electrons can freely move, resulting in higher electrical and thermal conductivity (Heintz, 1985, Miroshnichenko et al., 2023). Liquefaction not only increases the arrangement density of carbon atoms, but also promotes the flow of electrons, leading to an increase in conductivity. Moreover, due to the strong interaction between graphite

layers, heat can be efficiently conducted between these layers, thereby improving thermal conductivity.

In summary, there are significant differences in the characteristics of coke produced by thermal cracking and cooling. The coking rate gradually increases with the decrease of condensation temperature during the cooling process, reaching a peak between 200 and 300 °C. The coke formed within this temperature range is mainly amorphous, with uneven distribution and high graphitization degree. Once the coke adheres to the pipe wall, it will have a significant impact on the stability of the system.

3.3. Influence factors

In this section, the main factors affecting coke formation during the cooling process were explored by combining experimental measurements with physical property calculations.

3.3.1. Molecular interactions

The molecular interactions include Van der Waals forces, hydrogen bonds, and covalent bonds (Murgich, 2002; Tsuzuki et al., 2000). In this study, molecular interactions mentioned mainly refer to the Van der Waals force. During the cooling process, the coking precursor molecules undergo liquefaction. The changes in the physical properties of the coking precursors after liquefaction can also affect the intermolecular forces, thereby influencing the coke formation. Based on the calculation methods in Section 2.3, combined with the mixing rule (see supplementary material), the viscosity and density of the coking precursors can be obtained as a function of temperature.

The results show that whether it is a pure substance or a mixture. As the temperature approaches the liquefaction temperature of the coking precursors, both viscosity and density increase significantly. The increase in density and viscosity slows down molecular movement, resulting in longer residence time and enhancing the likelihood of molecular interactions and aggregation. The slow molecular motion helps the molecules to contact and aggregate more easily into larger molecular groups or aggregates, which are then deposited on the tube walls when reaching a certain size.

The saturated vapor pressure (p_{vp}) of major coking precursors as a function of temperature at the system pressure (p_{system}) of 3.5 MPa is illustrated in Fig. 7(c). When p_{system} is less than p_{vp}, the liquid tends to evaporate, reducing intermolecular aggregation and leading to a decrease in molecular interactions. However, during the cooling process, as the temperature decreases, the saturated vapor pressure also diminishes accordingly. When p_{system} is higher than p_{vp}, the vapor is in an unstable state, with part of the gas tending to condense to a saturated state, which promotes intermolecular aggregation and enhances the molecular interactions. Particularly, the more obvious the supersaturation state, the stronger the effect of molecular aggregation.

Overall, the liquefaction of coking precursor molecules during the cooling process has changes in physical properties that affect molecular aggregation (see Fig. 8). The increase in viscosity and density leads to an increase in the residence time of molecules. At the same time, liquefaction reduces the degree of disorder in the system, increases intermolecular forces and the tendency of polymerization, affects the structure and morphology of aggregates, thereby promoting the process of molecular aggregation and nucleation.

3.3.2. Molecular thermal motion

The influence of molecular thermal motion on molecular aggregation is both complex and variable. Under specific conditions, it can facilitate contact and aggregation between molecules, but

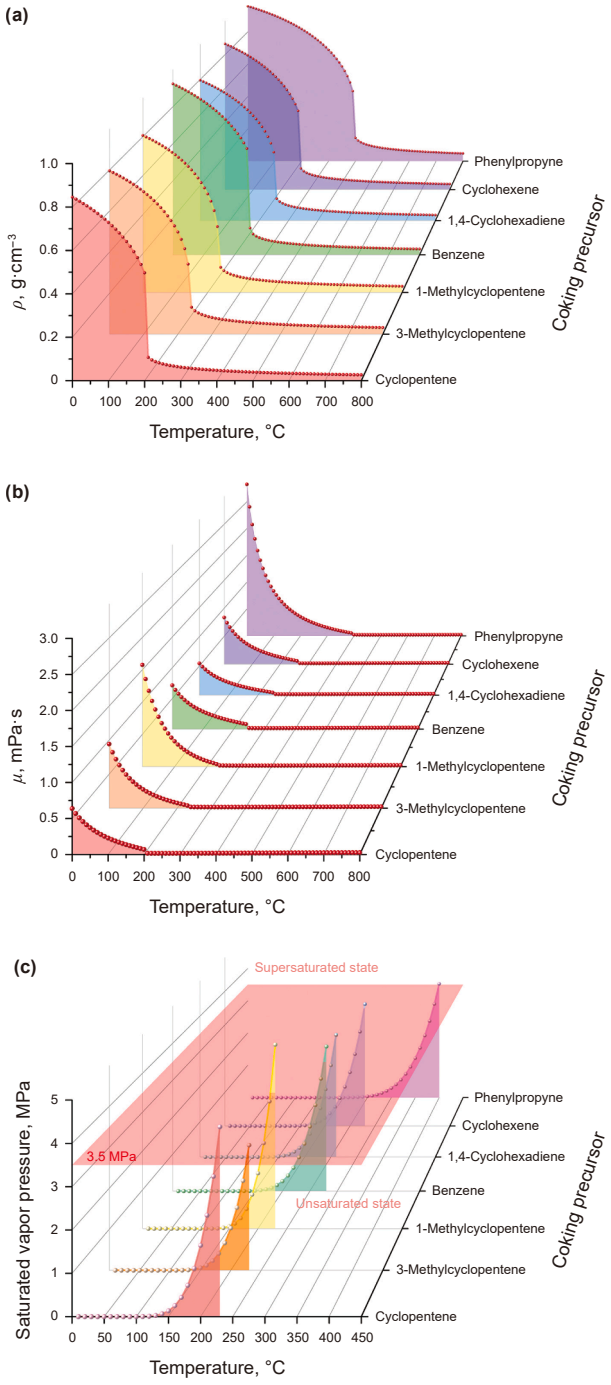

Fig. 7. Changes in physical parameters of coking precursors at different temperatures: **(a)** density; **(b)** viscosity; **(c)** material saturated vapor pressure.

also hinder the formation of stable aggregates due to excessive and vigorous motion (Yuan and Wu, 2022). The collision frequency, a physical quantity indicating the intensity of the thermal motion of reactive molecules, is given by a formula that shows:

$$\overline{Z} = \sqrt{2} n \bar{v} \pi d^2 \tag{19}$$

As temperature increases, the average velocity of molecules also increases, thereby increasing the collision frequency and the possibility of molecules aggregation through physical forces. However, the rise in temperature also intensifies the thermal

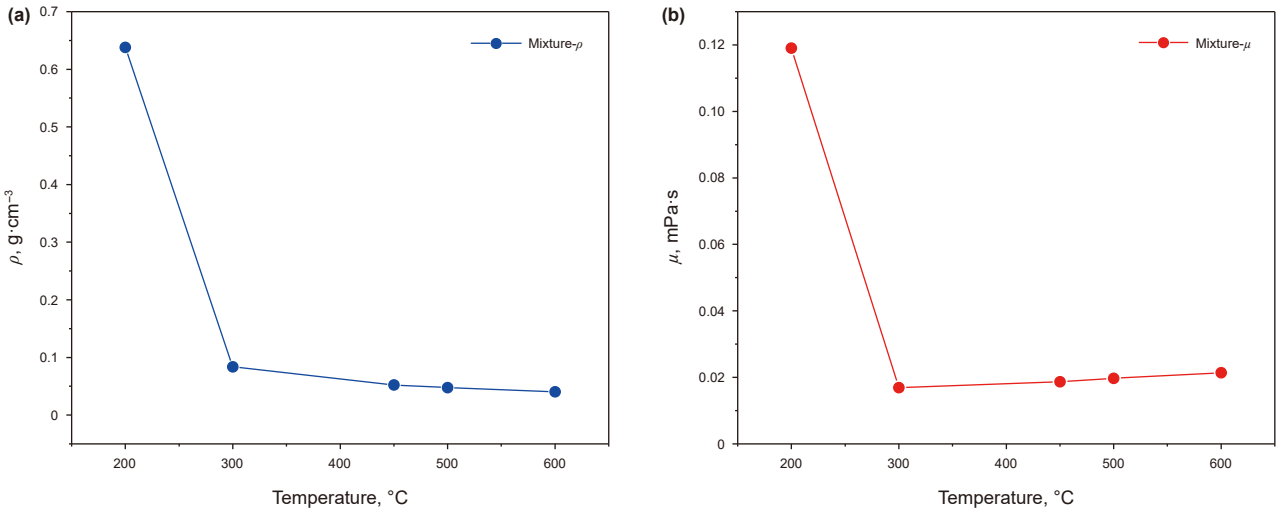

Fig. 8. Changes in physical properties of coking precursors after mixing in experiments: **(a)** density; **(b)** viscosity.

motion of molecules, which affects the aggregation and even hinders the formation of aggregates.

The two main factors influencing molecular aggregation are intermolecular forces and thermal motion. There exists a paradoxical relationship between the two factors. On the one hand, intermolecular forces encourage molecules to cluster together; on the other hand, thermal motion tends to drive them apart. The group contribution method was used to calculate the critical properties of different coking precursor molecules. By comparing the changes in viscosity, density, and saturated vapor pressure of precursors, it was found that the critical temperature of coking precursors is the main factor determining the molecular nucleation mode. In addition, molecular dynamics simulations were used to simulate the cooling process of benzene molecules through LAMMPS software, as shown in Fig. S3. It was found that the critical temperature is a key parameter that affects molecular interactions and molecular thermal motion by tracking the changes in density, potential energy, and kinetic energy of benzene.

When the temperature exceeds the critical temperature of the coking precursor, molecular motion becomes stronger, resulting in higher collision frequencies and weaker intermolecular forces. The phenomenon of molecular aggregation is not obvious. When the temperature is lower than the critical temperature of the coking precursor, both viscosity and density increase. As the potential energy increases, the molecular kinetic energy gradually decreases and falls below the potential energy. This means that intermolecular forces are enhanced, promoting the formation of larger molecular aggregates. When the cluster size is large enough, coke will be produced. The temperature determines the contribution of both to condensation coking, thereby affecting the formation and growth of coke.

3.4. Condensation coking mechanism

Research on coking characteristics during the cooling process indicates that the formation process and properties are significantly different from that of coke produced at high temperatures. It can be seen that temperature is a key factor affecting the pathway of coke formation. According to the experimental results and critical physical property calculations of coking precursors, the nucleation process can be roughly divided into three regions: (i) physical nucleation (white), (ii) non nucleation (light purple), and (iii) chemical nucleation (deep purple), as shown in Fig. 9.

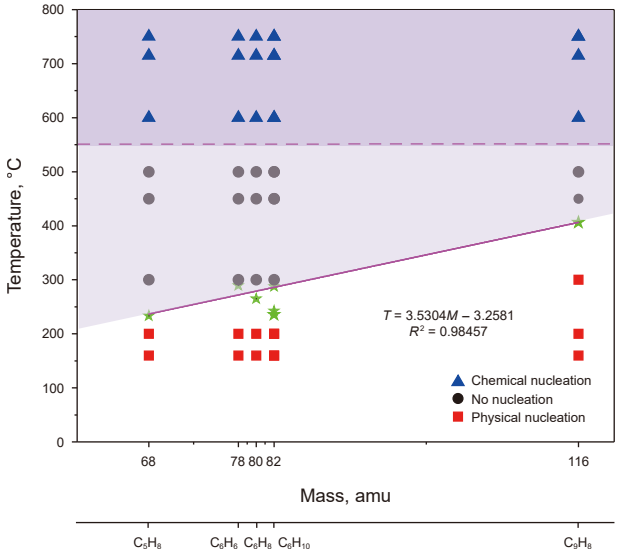

Fig. 9. Nucleation pathways of coke formed by different coking precursors at different temperatures.

When the temperature is above 500 °C, the formation and growth of coke mainly occur through chemical nucleation. Nucleation essentially does not occur between the temperature of 400 and 500 °C, due to the equilibrium state of molecular thermodynamics and kinetics. As the temperature decreases below 400 °C, the formation and growth of coke mainly proceed through physical nucleation. The green pentagram and purple solid line are the critical temperatures and simulated lines of coking precursors obtained through the group contribution method, while the purple dashed line is the approximate initial cracking temperature of *n*-decane obtained based on experimental data.

Based on extensive experimental research, nucleation is considered an important process for the generation and further growth of coke. Combining experimental results and theoretical analysis, the coking mechanism during the cooling process is proposed, as shown in Fig. 10.

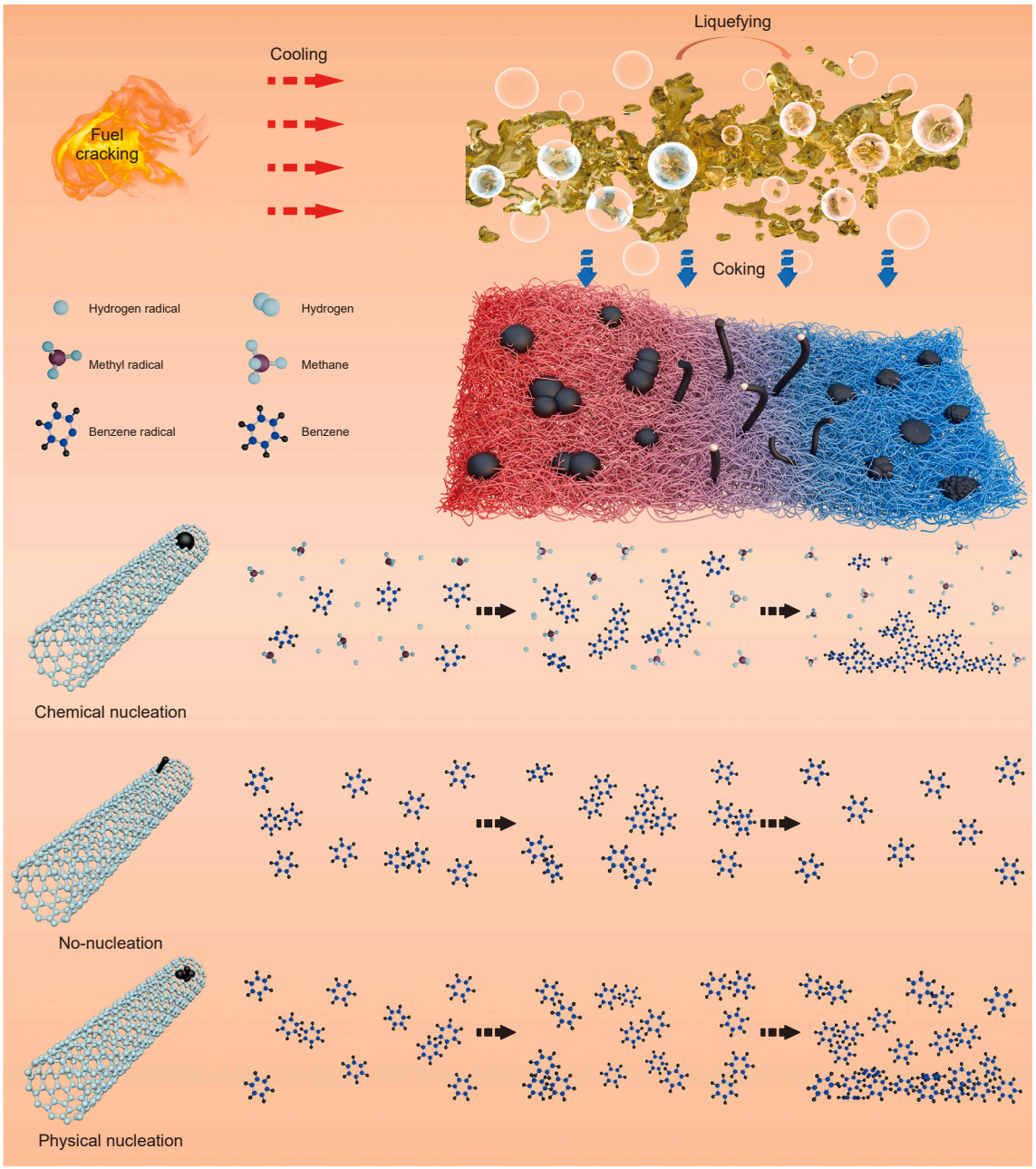

Fig. 10. Coking mechanism of endothermic hydrocarbon fuel during cooling process.

When the condensation temperature is high, small molecular free radicals and coking precursors undergo hydrogen abstraction reactions to generate polycyclic aromatic hydrocarbons. Then they form spherical coke on the substrate surface. As the condensation temperature decreases, molecules form dimers/trimers due to thermal collision. However, these aggregates are quite unstable easily dissolve in collisions with other monomers due to the intensity of thermal motion, hence most of them exist in the form of monomers.

When the condensation temperature is lower, this is also the difference from the coke produced at high temperatures. The nucleation process of coke is divided into three parts: pre-nucleation, mid-nucleation, and post-nucleation. In the pre-nucleation stage, as the temperature decreases, the physical properties of coking precursors begin to change, inducing a phase transition in the molecules. The physical forces between molecules cause them to randomly and freely aggregate, forming small dimers or trimers molecular clusters. In the mid-nucleation stage, which is the critical nucleation stage, the molecular clusters reach a certain critical size and become stable enough to continue attracting more molecules, thus forming stable aggregates. In the post-nucleation stage, the stable nuclei formed continue to attract surrounding molecules, promoting cluster growth. Once the size of the molecular clusters increases to a certain extent, the clusters rapidly deposit on the tube walls, forming the amorphous coke.

In general, the aggregation and deposition mechanism of incipient coke particles induced by condensation during the pyrolysis of hydrocarbon fuels can be obtained. When the coking precursor entering the cooling process, the average thermal motion rate and kinetic energy between molecules are reduced due to

the decrease in temperature. The interaction between molecules gradually becomes significant, and there is a trend of attraction and proximity between molecules. As the maximum liquefaction temperature approaches, some molecules begin to form aggregates or cores in a supersaturated state. Under the influence of intermolecular forces and thermal motion, the aggregates continuously form and dissociate until reaching an equilibrium state. After the temperature continues to decrease below the maximum liquefaction temperature, the molecules begin to liquefy, and the attraction between molecules is strong enough to overcome the thermal motion between molecules. At the same time, the physical properties of molecules, such as density, viscosity, and saturated vapor pressure, change towards the direction of molecular aggregation, making the interactions between molecules stronger and continuously allowing molecules to enter the aggregates. As the temperature further decreases, aggregates continue to grow and aggregate. When the size and stability of aggregates reach a certain level, they deposit on the pipe wall to form coke.

4. Conclusion

The condensation coking characteristics was investigated by controlling the cooling process. The experimental results indicate that there is a significant difference in the coking characteristics between condensation and thermal cracking. The gas yield and conversion of fuel increase with the decrease of condensation temperature, reaching 70.86% and 88.97% at 200 °C, 71.42% and 89.75% at 300 °C, respectively. At the same time, the mass fraction of the main coking precursor also increases to 55% at lower condensation temperatures. In addition, the coking rate gradually increases with the decreasing condensation temperature, reaching the peak of approximately 0.102 $mg{\cdot}cm^{-2}{\cdot}s^{-1}$ between 200 and 300 °C. The amorphous coke formed in this temperature range has the characteristics of uneven distribution and high graphitization degree.

The aggregation and deposition mechanism of incipient coke particles induced by condensation during the fuel pyrolysis is proposed with the experimental results and theoretical analysis. The decrease in temperature leads to the liquefaction of coking precursors, changes the physical properties, thereby enhancing the physical interactions between molecules. The molecules begin to aggregate to form molecular clusters, which deposits to form irregular coke reaching a certain size.

This work explains the reasons for pressure instability during the multiple cycles of heating and cooling process, providing theoretical support for the inhibition of condensation coking, which is beneficial for achieving the reuse of high-speed aircraft.

CRediT authorship contribution statement

Liu-Ru Liu: Methodology, Conceptualization, Investigation, Writing – original draft, Writing – review & editing, Software. **Yu Liu:** Investigation, Validation. **Lang Luo:** Investigation, Software. **Xin-Ke Wang:** Investigation. **Wen-Rui Yan:** Investigation. **Bo Wang:** Resources, Writing – review & editing, Project administration. **Quan Zhu:** Writing – review & editing, Project administration, Conceptualization, Resources.

Declaration of competing interest

The authors declare that they have no known competing financial interests or personal relationships that could have appeared to influence the work reported in this paper.

Acknowledgements

The authors gratefully acknowledge financial support from the National Natural Science Foundation of China (22308233, 92060101), the Natural Science Foundation of Sichuan Province of China (2024NSFSC1162), the Source of Origin Project of Beijing Power Machinery Research Institute, and the Sichuan Province Science Fund for Distinguished Young Scholars (2021JDJQ0011).

We would like to thank Yong Liu from the Analytical & Testing Center of Sichuan University for her help with the SEM measurements.

We sincerely thank Prof. Li Wu at Analytical & Testing Center of Sichuan University for the measurement of Raman.

Appendix A. Supplementary data

Supplementary data to this article can be found online at https://doi.org/10.1016/j.petsci.2025.08.019.

References

Abdalla, A., Ying, Y., Jiang, B., et al., 2020. Comparative study on characteristics of soot from *n*-decane and RP-3 kerosene normal/inverse diffusion flames. J. Energy Inst. 93 (1), 62–75. https://doi.org/10.1016/j.joei.2019.04.008.

Ambrose, D., Walton, J., 1989. Vapour pressures up to their critical temperatures of normal alkanes and 1-alkanols. Pure Appl. Chem. 61 (8), 1395–1403. https://doi.org/10.1351/pac198961081395.

Chen, L.L., Zhang, J., Li, C.G., et al., 2024. Regulating metal-acid double site balance on mesoporous SiO_2-Al_2O_3 composite oxide for supercritical n-decane cracking. Pet. Sci. 21 (4), 2881–2891. https://doi.org/10.1016/j.petsci.2024.02.005.

Chung, S., Violi, A., 2011. Peri-condensed aromatics with aliphatic chains as key intermediates for the nucleation of aromatic hydrocarbons. Proc. Combust. Inst. 33 (1), 693–700. https://doi.org/10.1016/j.proci.2010.06.038.

Chung, T., Lee, L., Starling, K., 1984. Applications of kinetic gas theories and multiparameter correlation for prediction of dilute gas viscosity and thermal conductivity. Ind. Eng. Chem. Fundam. 23 (1), 8–13. https://doi.org/10.1021/i100013a002.

Constantinou, L., Gani, R., 1994. New group contribution method for estimating properties of pure compounds. AIChE J. 40 (10), 1697–1710. https://doi.org/10.1002/aic.690401011.

DeWitt, M., Edwards, T., Shafer, L., et al., 2011. Effect of aviation fuel type on pyrolytic reactivity and deposition propensity under supercritical conditions. Ind. Eng. Chem. Res. 50 (18), 10434–10451. https://doi.org/10.1021/ie200257b.

Efimov, I., Gabdulkhakov, R., Rudko, V., 2024. Fine-tuned convolutional neural network as a tool for automatic microstructure analysis of petroleum and pitch cokes. Fuel 376, 132725. https://doi.org/10.1016/j.fuel.2024.132725.

Fedors, R., 1982. A relationship between chemical structure and the critical temperature. Chem. Eng. Commun. 16 (1–6), 149–151. https://doi.org/10.1080/00986448208911092.

Feng, Y., Cao, Y., Liu, S., et al., 2019. The influence of coking on heat transfer in turbulent reacting flow of supercritical hydrocarbon fuels. Int. J. Heat Mass Tran. 144, 118623. https://doi.org/10.1016/j.ijheatmasstransfer.2019.118623.

Gleason, K., Carbone, F., Sumner, A., et al., 2021. Small aromatic hydrocarbons control the onset of soot nucleation. Combust. Flame 223, 398–406. https://doi.org/10.1016/j.combustflame.2020.08.029.

Gong, X., Gao, Y., Wang, B., et al., 2023. The dominant role of surface chemistry on coking resistance of passivating coating. Appl. Energy 352, 121929. https://doi.org/10.1016/j.apenergy.2023.121929.

Guisnet, M., Magnoux, P., 2001. Organic chemistry of coke formation. Appl. Catal. Gen. 212 (1), 83–96. https://doi.org/10.1016/S0926-860X(00)00845-0.

Heintz, E., 1985. Influence of coke structure on the properties of the carbon-graphite artefact. Fuel 64 (9), 1192–1196. https://doi.org/10.1016/0016-2361(85)90173-5.

Huang, L., Huang, S., Mao, Y., et al., 2023. An experimental study on the laminar burning velocities of RP-3 kerosene and its surrogate fuel at elevated pressures and temperatures. Fuel 331, 125844. https://doi.org/10.1016/j.fuel.2022.125844.

Jia, Z., Huang, H., Zhou, W., et al., 2014. Experimental and modeling investigation of *n*-decane pyrolysis at supercritical pressures. Energy Fuels 28 (9), 6019–6028. https://doi.org/10.1021/ef5009314.

Joback, K., Reid, R., 1987. Estimation of pure-component properties from group-contributions. Chem. Eng. Commun. 57 (1–6), 233–243. https://doi.org/10.1080/00986448708960487.

Khalaf, M., Mansoori, G., 2018. A new insight into asphaltenes aggregation onset at molecular level in crude oil (an MD simulation study). J. Petrol. Sci. Eng. 162, 244–250. https://doi.org/10.1016/j.petrol.2017.12.045.

Kim, J., Seo, J., Han, D., et al., 2022. Prediction of thermochemical and transport properties of hydrocarbon aviation fuel in supercritical state with thermal decomposition. Fuel 325, 124805. https://doi.org/10.1016/j.fuel.2022.124805.
Konda, S., Vuchuru, K., Nalabala, M., et al., 2022. Investigation of heat sink, coke deposition, and cracking characteristics of C7 paraffin, cycloparaffin, and aromatic hydrocarbons under supercritical conditions. J. Supercrit. Fluids 191, 105757. https://doi.org/10.1016/j.supflu.2022.105757.
Litvinova, T., Tsareva, A., Poltoratskaya, M., et al., 2024. The mechanism and thermodynamics of ethyl alcohol sorption process on activated petroleum coke. J. Mining Inst. (268), 625–636.
Liu, X., Zhu, H., Li, S., et al., 2023. Effect of temperature on the aggregation kinetic and interaction mode of asphaltene in toluene-heptane system at molecular level using molecular dynamics (MD) simulation. J. Mol. Liq. 384, 122167. https://doi.org/10.1016/j.molliq.2023.122167.
Liu, Z., Pan, H., Feng, S., et al., 2015. Dynamic behaviors of coking process during pyrolysis of China aviation kerosene RP-3. Appl. Therm. Eng. 91, 408–416. https://doi.org/10.1016/j.applthermaleng.2015.08.033.
Liu, Z., Yuan, S., Gong, S., et al., 2021. Long-term thermal oxidative deposition of RP-3 jet fuels: mechanism and modeling. Fuel 303, 121250. https://doi.org/10.1016/j.fuel.2021.121250.
Luo, S., Xu, D., Song, J., et al., 2021. A review of regenerative cooling technologies for scramjets. Appl. Therm. Eng. 190, 116754. https://doi.org/10.1016/j.applthermaleng.2021.116754.
Mao, Q., van, A., Luo, K., 2017. Formation of incipient soot particles from polycyclic aromatic hydrocarbons: a ReaxFF molecular dynamics study. Carbon 121, 380–388. https://doi.org/10.1016/j.carbon.2017.06.009.
Mao, Y., Yu, L., Wu, Z., et al., 2019. Experimental and kinetic modeling study of ignition characteristics of RP-3 kerosene over low-to-high temperature ranges in a heated rapid compression machine and a heated shock tube. Combust. Flame 203, 157–169. https://doi.org/10.1016/j.combustflame.2019.02.015.
Miroshnichenko, D., Shmeltser, K., Kormer, M., 2023. Factors affecting the formation the carbon structure of coke and the method of stabilizing its physical and mechanical properties. C-Journal of Carbon Research 9 (3), 66. https://doi.org/10.3390/c9030066.
Morán, J., Henry, C., Poux, A., et al., 2021. Impact of the maturation process on soot particle aggregation kinetics and morphology. Carbon 182, 837–846. https://doi.org/10.1016/j.carbon.2021.06.085.
Murgich, J., 2002. Intermolecular forces in aggregates of asphaltenes and resins. Petrol. Sci. Technol. 20 (9–10), 983–997. https://doi.org/10.1016/0016-2361(85)90173-5.
Ning, W., Yu, P., Jin, Z., 2013. Research status of active cooling of endothermic hydrocarbon fueled scramjet engine. J. Aero. Eng. 227 (11), 1780–1794. https://doi.org/10.1177/0954410012463642.
Peng, D., Robinson, D., 1976. A new two-constant equation of state. Ind. Eng. Chem. Fundam. 15 (1), 59–64. https://doi.org/10.1021/i160057a011.
Richter, H., Howard, J., 2000. Formation of polycyclic aromatic hydrocarbons and their growth to Soot—a review of chemical reaction pathways. Prog. Energy Combust. Sci. 26 (4–6), 565–608. https://doi.org/10.1016/S0360-1285(00)00009-5.
Sharikov, F., Rudko, V., Smyshlyaeva, K., 2023. Oxidation thermolysis kinetics of asphaltenes with various chemical prehistory. Thermochim. Acta 726, 179550. https://doi.org/10.1016/j.tca.2023.179550.
Sharma, A., Mukut, K., Roy, S., et al., 2021. The coalescence of incipient soot clusters. Carbon 180, 215–225. https://doi.org/10.1016/j.carbon.2021.04.065.
Shukla, B., Koshi, M., 2012. A novel route for PAH growth in HACA based mechanisms. Combust. Flame 159 (12), 3589–3596. https://doi.org/10.1016/j.combustflame.2012.08.007.
Song, T., Lan, Z., Ma, X., et al., 2009. Molecular clustering physical model of steam condensation and the experimental study on the initial droplet size distribution. Int. J. Therm. Sci. 48 (12), 2228–2236. https://doi.org/10.1016/j.ijthermalsci.2009.05.004.
Sun, D., Du, Y., Zhang, J., et al., 2017. Effects of molecular structures on the pyrolysis and anti-coking performance of alkanes for thermal management. Fuel 194, 266–273. https://doi.org/10.1016/j.fuel.2016.12.090.
Tsuzuki, S., Honda, K., Uchimaru, T., et al., 2000. The magnitude of the CH/π interaction between benzene and some model hydrocarbons. J. Am. Chem. Soc. 122 (15), 3746–3753. https://doi.org/10.1021/ja993972j.
Van, B., Holle, E., Florijn, J., 2013. The use of pyrolysis oil and pyrolysis oil derived fuels in diesel engines for CHP applications. Appl. Energy 102, 190–197. https://doi.org/10.1016/j.apenergy.2012.05.047.
Vandewiele, N., Magoon, G., Van, K., et al., 2014. Kinetic modeling of jet propellant-10 pyrolysis. Energy Fuels 29 (1), 413–427. https://doi.org/10.1021/ef502274r.
Vuchuru, K., Dinda, S., Surasani, V.K., 2023. Development of coke model for thermal cracking of hydrocarbon fuels under supercritical conditions and its experimental validation. J. Anal. Appl. Pyrolysis 173, 106079. https://doi.org/10.1016/j.jaap.2023.106079.
Wang, N., Wang, L., Zhi, Y., et al., 2023. Coking and decoking chemistry for resource utilization of polycyclic aromatic hydrocarbons (PAHs) and low-carbon process. J. Energy Chem. 76, 105–116. https://doi.org/10.1016/j.jechem.2022.09.014.
Wang, X., Yan, W., Pan, J., et al., 2025. Effects of the mixing ratios of n-decane/methylcyclohexane binary fuel on the thermal cracking and carbon deposition propensity. Int. J. Heat Mass Tran. 238, 126–481. https://doi.org/10.1016/j.ijheatmasstransfer.2024.126481.
Wang, Y., Cheng, Y., Li, M., et al., 2021a. Experimental and theoretical modeling of the effects of pressure and secondary reactions on pyrolysis of JP-10 at supercritical pressures. Fuel 306, 121737. https://doi.org/10.1016/j.fuel.2021.121737.
Wang, Y., Gu, M., Wu, J., et al., 2021b. Formation of soot particles in methane and ethylene combustion: a reactive molecular dynamics study. Int. J. Hydrogen Energy 46 (73), 36557–36568. https://doi.org/10.1016/j.ijhydene.2021.08.125.
Wang, Z., Wang, B., Li, Q., et al., 2024. Effect of ethane on condensation characteristics of methane heterogeneous nucleation: a molecular dynamics study. Fuel 358, 130182. https://doi.org/10.1016/j.fuel.2023.130182.
Xiong, Z., Syed-Hassan, S., Hu, X., et al., 2019. Pyrolysis of the aromatic-poor and aromatic-rich fractions of bio-oil: characterization of coke structure and elucidation of coke formation mechanism. Appl. Energy 239, 981–990. https://doi.org/10.1016/j.apenergy.2019.01.253.
Yan, W., Wang, X., Dong, J., et al., 2024. Role of ammonia addition on the growth of polycyclic aromatic hydrocarbon and coke surface at deep cracking of endothermic hydrocarbon fuels. Chem. Eng. J. 496, 154015. https://doi.org/10.1016/j.cej.2024.154015.
Yin, Z., Liu, S., Tan, D., et al., 2023. A review of the development and application of soot modelling for modern diesel engines and the soot modelling for different fuels. Process Saf. Environ. Prot. 178, 836–859. https://doi.org/10.1016/j.psep.2023.08.075.
Yu, P., Liu, X., Zhu, H., et al., 2023. Effect of cooling rates on aggregation interaction of asphaltene molecules: insights from molecular dynamics simulations. Colloids Surf. A Physicochem. Eng. Asp. 679, 132632. https://doi.org/10.1016/j.colsurfa.2023.132632.
Yuan, H., Kong, W., Liu, F., et al., 2019. Study on soot nucleation and growth from PAHs and some reactive species at flame temperatures by ReaxFF molecular dynamics. Chem. Eng. Sci. 195, 748–757. https://doi.org/10.1016/j.ces.2018.10.020.
Yuan, R., Wu, L., 2022. Capturing the influence of intermolecular potential in rarefied gas flows by a kinetic model with velocity-dependent collision frequency. J. Fluid Mech. 942. https://doi.org/10.1017/jfm.2022.350.
Zhang, H., Li, W., Nian, Y., et al., 2024. Insights into the pyrolytic coking process of RP-3 fuel from ReaxFF molecular dynamics. Chem. Eng. Sci. 291, 119935. https://doi.org/10.1016/j.ces.2024.119935.
Zhang, X., Di, N., Xu, L., et al., 2023. Study on the formation process of soot from 2,5-dimethylfuran pyrolysis by ReaxFF molecular dynamics. J. Therm. Anal. Calorim. 148 (17), 9145–9166. https://doi.org/10.1007/s10973-023-12301-2.
Zhao, S., Pu, W.F., Su, L., et al., 2021. Properties, combustion behavior, and kinetic triplets of coke produced by low-temperature oxidation and pyrolysis: implications for heavy oil in-situ combustion. Pet. Sci. 18 (5), 1483–1491. https://doi.org/10.1016/j.petsci.2021.08.005.
Zhu, Y., Yan, S., Zhao, R., et al., 2018. Experimental investigation of flow coking and coke deposition of supercritical hydrocarbon fuels in porous media. Energy Fuels 32 (3), 2941–2948. https://doi.org/10.1021/acs.energyfuels.7b03436.